Please cite this work as:

Magar, V. (2020) *Sediment transport and morphodynamic modelling for coasts and shallow environments*. First Edition. Boca Raton, Florida: CRC Press. ISBN: 9781498753463. 216pp. *In Press*.

Sediment transport and morphodynamic modelling for coasts and shallow environments

Vanesa Magar

November 11, 2019

Contents

Preface

When Tony Moore from CRC Press came to see me back in 2011 and suggested I write a book, I had to ponder this for some time. After several months, I decided to send him a book proposal on sediment transport and morphodynamic modelling in coastal environments, to see whether he would agree. The book proposal was, in general, well received by Tony and the reviewers, but most importantly, Tony was confident I could undertake this project to completion. I invited a senior researcher, Prof. Alan G. Davies, with whom I had collaborated during the SANDPIT project (EC Framework V Project Contract no. EVK3-2001-00056), to be a co-author. But Alan was also confident I could undertake this without much additional input. Thus, in 2015, I signed the contract with CRC Press and embarked on this adventure. Initially, Tony was giving a lot of advice to help me organize my time so that I would finish in two years. However, it took a bit longer than that, not by lack of interest but lack of time. In 2015, I had moved back to Mexico and was involved in several renewable energy projects. Our work required a certain level of social activism, with some focus on marine spatial planning and management, while trying to influence national policies. Such a turn in my career was due to a realization that we needed to take urgent climate change action. We were endangering all forms of life with our anthropogenic activities and greenhouse gas emissions. We needed, therefore, to focus on projects of significant benefit for the Planet and our environment. Some of these worries have affected how I wrote this book. Also, they influenced the selection of pressing issues to address, presented in the final chapters. I have, however, been relatively loyal to the original content plan.

Although the book is mostly a research monograph, I hope it is of interest to researchers and practitioners alike. A strong focus is on the dynamics of coastal environments at different scales and under a variety of forcings, using models, in-situ data, and remote sensing techniques. A broad overview of the different chapters is as follows. Chapter 1 briefly defines different spatio-temporal scales, as well as several essential terms and concepts. We present linkages with modern observation tools and regional models and introduce definitions and concepts related to coastal management. These concepts and tools may be used to solve endless research

questions and provide interesting discussions. They are essential for the analysis of the physics and the dynamics, but also for assessing biogeochemical and ecological problems, and for communication with colleagues, authorities, or other interested parties. Chapter 2 provides essential information on the physics of open coasts and sheltered environments, including grain size distributions, sediment composition, bottom boundary layer dynamics, wave and tidal dynamics, and their effects on sediment transport and morphodynamic modelling, the main focus of this work. Chapter 3 then introduces basic and advanced regional modelling tools. We attempt here to guide best practices, for example, on grid generation, bathymetry interpolations, methods of solution. The chapter also covers different types of modelling approaches in wave-dominated and in sheltered environments. Data-driven methods are also discussed, as such decompositions into a small number of dominant patterns can be very useful to understand long-term dynamics. Finally, Chapter 4 provides detailed descriptions of typical applications of regional models, including estuarine dynamics, shoreline evolution, and environmental impacts of offshore structures.

I would like to thank those who have made this project possible. First, thanks to CRC Press, whose support has been instrumental. I was glad to have them touching base from time to time, and checking whether the draft was (or not) making any progress. As the bulk of the book took shape, I benefited significantly from Alan's thorough reviews, in particular, his comments about adding examples and important results. Thank you, Alan, for all the time you invested in the past year to this project. I learnt how to synthesize well essential results after I read the book edited by Reginald Uncles and Steven Mitchell; that book was extremely valuable during the revisions of this work. I amply recommend it to anyone interested in these topics.

Thanks to Anahí Bermúdez Romero and Victor Manuel Godínez Sandoval for your help with the figures and schematics reproduced in the text. Thank you as well for looking after important deliverables in other projects, while I worked on this book. Finally, thanks to my husband and co-leader of the GEM*lab*, Markus Gross, and to our son Damián Gross-Magar, for their patience.

Dedicated to those pursuing greater purpose and goodness in life, despite hostilities and pressures.

Ensenada, Mexico, 18 July 2019.

Chapter 1

Introduction

Coasts and shallow coastal environments evolve in response to different forcings and constraints, for example: the supply of sediment; the action of winds, waves, currents, and density gradients; the effects of extreme events such as hurricanes, tsunamis and landslides; the presence of beaches, dunes, coastal lagoons, estuaries or deltas; and the changes induced by human intervention and global warming on the coast. These forcings and constraints act at different space and time scales. Large spatio-temporal scales provide the boundary conditions for a model that can generate the small spatio-temporal scales and, in turn, the physics resolved at small spatio-temporal scales are parameterized in models at large spatio-temporal scales (Brommer & Bochev-Van Der Burgh 2009). Thus, there is an exchange of matter, momentum and energy between scales, known as the *cascade hierarchy* (Cowell et al. 2003). Moreover, processes and bedforms at a same spatio-temporal scale are linked to one another through dynamic interactions; this is known as the *primary scale relationship* (de Vriend 1991). A schematic of the cascade hierarchy is shown in fig. 1.1. The space and timescales shown are in orders of magnitude only, implying that there is some flexibility on the boundary limits for the scale boxes shown, depending on the circumstances - for example, under extreme events, or long recovery time periods. We will now discuss in more detail the primary scale relationships in the context of coastal geomorphology and dynamics, or coastal morphodynamics.

1.1 Physics and modelling at different scales

The study of coastal morphodynamics involves investigating the changes to the physical processes and bedforms in the coastal environment over a broad range of scales in space and time, from the microscale to the

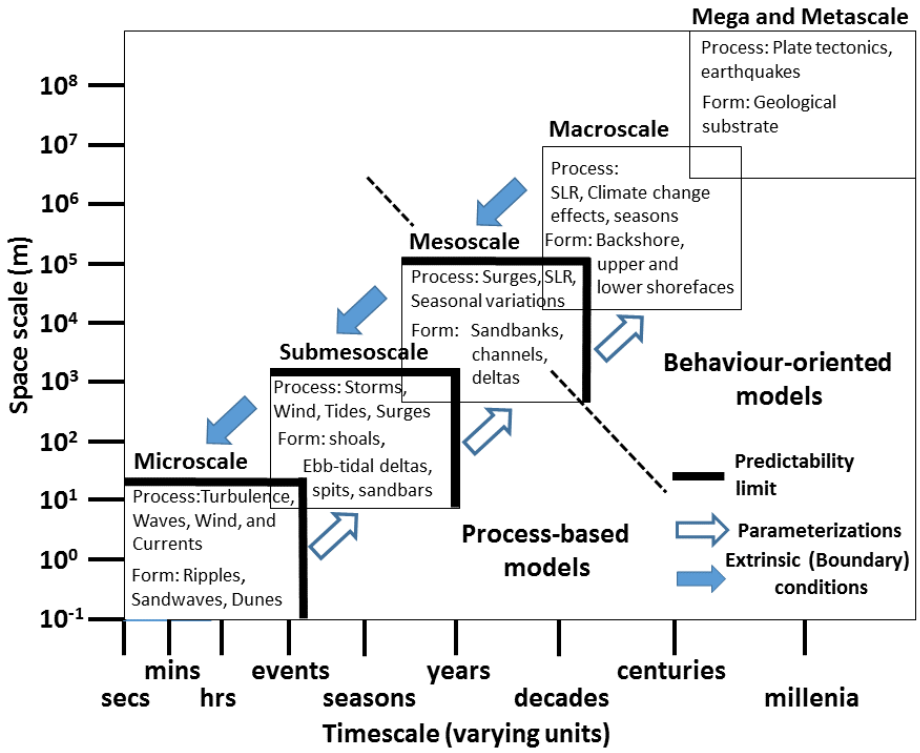

Figure 1.1: Cascade hierarchy of spatio-temporal scales, after Brommer & Bochev-Van Der Burgh (2009).

macroscale. The motions near the bed are crucial as the bed is one of the most important sources of sediment, together with bedform migration and estuarine discharges. Sediments transported by the flow may be divided into three different transport types depending on their median grain diameter and their dynamics: bedload, suspended load and wash load. The differences between these three types of sediment load will be explained in Sec. 1.1.1, on microscale processes. The types and concentrations of the sediments will strongly depend on the coastal environment, which may be classified into three simple types: sandy or pebbled coasts, erodible or non-erodible bluffs and cliffs, or sheltered low-lying lands and estuaries. Such environments may extend from tens, to hundreds, to thousands of meters, and therefore may be affected by submesoscale, mesoscale, or macroscale processes. The US federal emergency management agency (FEMA) defines six different beach settings, representative of the settings generally found on the Pacific Coast of the US, according to their morphology and vulnerability to storms (FEMA 2015):

1. Sandy beaches backed by low sand berms or high sand dune formations

2. Sandy beaches backed by shore protection structures

3. Cobbled, gravelly, shingle, or mixed grain sized beaches and berms

4. Erodible coastal bluffs

5. Non-erodible coastal bluffs or cliffs

6. Tidal flats, coastal lagoons, wetlands, and other reduced energy basins

with beach settings 1 to 3 corresponding to open beaches, beach settings 4 and 5 corresponding to bluffs and cliffs, and beach setting 6 corresponding to low-lying sheltered environments. The extent of the study domain and the resolution at which one is carrying out a study clearly affect the scale of the processes that need to be considered. For consistency, it is therefore very useful to identify the morphological and dynamical mechanisms that affect the evolution of different coastal environments at different scales.

1.1.1 Microscale

The bottom boundary layer of the nearshore region is governed by microscale processes and bedforms. At the very low end of the microscale, at lengthscales below O(0.1) m and timescales of the order of seconds, turbulence and individual particle motions are the dominant processes. Bedload differs from suspended load in that the bedload sediment particles remain close to the seabed and move by traction or saltation. Traction occurs when the sediment and the fluid have comparable densities, while saltation is common when the particle density is large in comparison to that of the surrounding fluid (Charru et al. 2013). When studying bedload transport, it is important to consider the threshold of motion of the sediment, which occurs at Shields numbers, θ, equal to the critical Shields number, θ_c. The Shields number is a dimensionless shear stress, and depends on the geometry of the grains (whether they are smooth or rough), the fluid viscosity, the fluid and the particle densities, the median grain diameter, and the friction velocity at the seabed. The threshold of motion may also be defined in terms of excess pressure gradients, through the Sleath parameter (Sleath 1982). More formal definitions of the boundary shear stress, the Sleath parameter, and the boundary Reynolds number, will be provided in Chap. 2. Once the shear stresses generate a lifting force that is large in comparison to the particles' stabilizing forces, bedload sediments start rolling or hopping on the bed, moving by traction or saltation. Once turbulent forces are large enough to lift the sediment higher into the water column, the bedload turns into suspended load, and the particles are advected by the main flow. This occurs when the fluid velocity fluctuations become comparable, in magnitude, to the sediment settling velocity. In other words, the balance between erosion and deposition depends on the flow speed near the bed and the sediment median grain diameter (Hjulstroöm 1935). Materials in suspension are maintained as suspended load by turbulent motion (Bagnold 1966); they may have come from upstream reaches, carried downstream as wash load. Wash load sediments are fine particles such as clays, silts or very fine sands, with very small

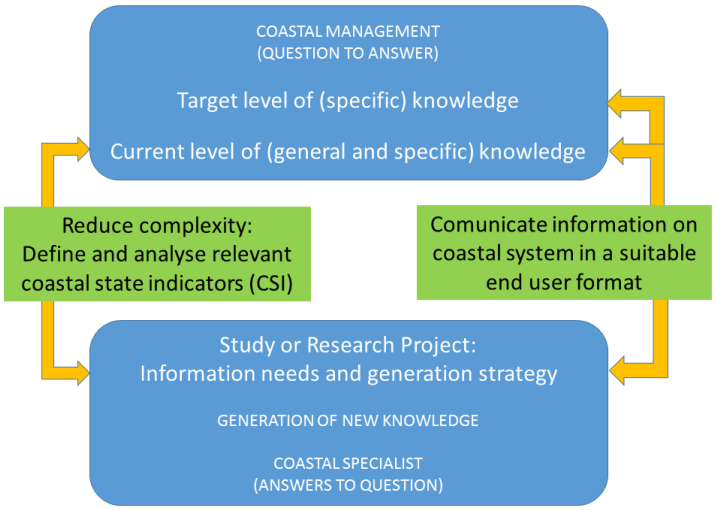

Figure 1.7: "Innovative" communication strategy, based on Van Rijn et al. (2005) and Van Koningsveld et al. (2005).

be derived from video or satellite imagery, from oceanographic and coastal measurements, from laboratory observations, or from numerical models.

A generic approach for identifying essential CSIs, based either on the needs of short, medium and long-term management practice and innovation was proposed by Van Koningsveld et al. (2005). As a first step, "problem-driven" CSIs are chosen within a management context and key issues are identified and posed as questions that coastal managers need to be asking about their site. Then, as a second step, each field site is assessed scientifically using a systems-driven approach, to define a set of "systems-driven" CSIs; these are indicators, or predictors, of known dynamic elements of the coastal system. If an emerging new technology is used during the scientific exploration of the site, then such techniques may lead to novel predictors describing the site dynamics. The problem-driven and system-driven CSIs should be comparable. As a third step, CSIs are selected depending on whether they help end users address a particular associated question. The final set of CSIs is reported and presented to coastal managers in an end user-friendly format. The process requires a series of end user-specialist discussions before an agreement is reached.

1.3 How this book is organized

As mentioned above, there are still important questions to address on sediment transport and coastal morphodynamic modelling in nearshore environments, and some of them will become evident throughout the book. This monograph will provide a comprehensive synthesis of state-of-the-art research and development,

with worked examples in simple scenarios.

Chapter 2 covers the fundamental hydrodynamics of estuarine and coastal environments, properties of seafloor and estuarine composition, and hydro-environmental interactions. Emphasis is placed on the feedbacks between small and large scale processes, and between short and large evolution timescales. The theory is placed within the context of current and emerging soft engineering approaches for coastal management and protection, in particular on managed realignment, coastal protection and climate change.

Chapter 3 follows with an in-depth coverage of numerical modelling techniques, where the challenges imposed by the modelling at multiple scales and the coupling of the physics with the dynamics is emphasized. Detail on how to configure regional models for typical and advanced coastal engineering applications is provided. The book covers a wide range of environments, but particularly those for which shallow water theory is applicable. Coupling of the models with surface waves is discussed, and case studies where waves are of importance are included.

Chapter 4 focuses on current and future model applications with an emphasis on climate change. Topics covered include storm surge and inundation modelling, shoreline management and coastal erosion, the sand engine case study of morphodynamic modelling for beach renourishment schemes, and a closing section on offshore renewable energy.

Chapter 2

Fundamental Physics of Estuaries and Shallow Coastal Environments

2.1 Threshold of motion

Erodible beds in sea shores and river deltas provide the necessary sediments for natural coastal accretion throughout the world. Such erodible beds may have different compositions and percentage content of different sediment sizes, and these sizes and material types in turn determine the degree of cohesiveness or non-cohesiveness of the bed. A typical coarse (i.e., non detailed) sediment size classification scheme is shown in diagram 2.1, where the sediments have been divided into only three types: mud (which may be divided into clay and silt), sand and gravel (van Maren 2009). The nominal particle sizes shown in the diagram follow Wentworth's grade scale. With these three types, bed compositions can be classified into fifteen major, 3-way textural sediment groups, which can be very clearly represented in the form of a sectioned triangle, as shown in Fig. 2.2. Another sectioned triangle may be defined for clay-silt-sand mixtures, as shown in Fig. 2.3. The textural classification of sand-silt-clay shows that mud has a silt:clay fraction between 2:1 and 1:2, while silts have at least a 2:1 silt:clay fraction and clays at least a 1:2 silt:clay fraction.

A detailed classification of sediments with size larger than the nominal size for gravel, would require perhaps a third gravel-cobble-boulder triangle for seabeds with a large content of gravel, cobbles and boulders. Such a classification could be relevant in very energetic regions with a cobbled seabed. Some of these environments are found in high latitudes, for example in the Orkney Islands, U.K., or in rocky-cliffed regions where a large

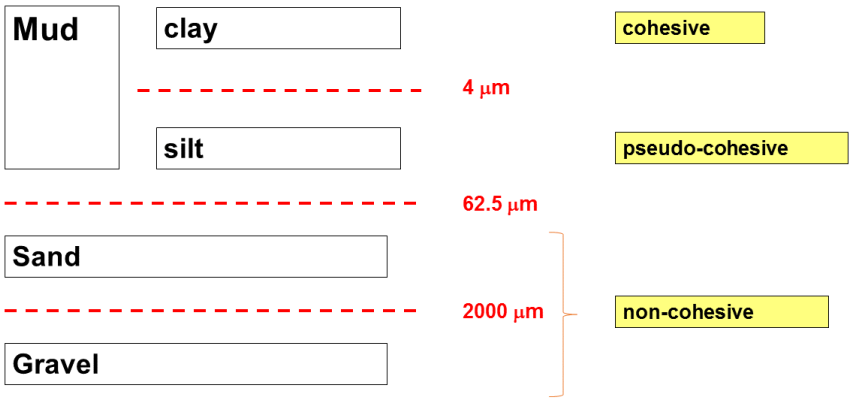

Figure 2.1: Sediment size schematic, after van Maren (2009)

.

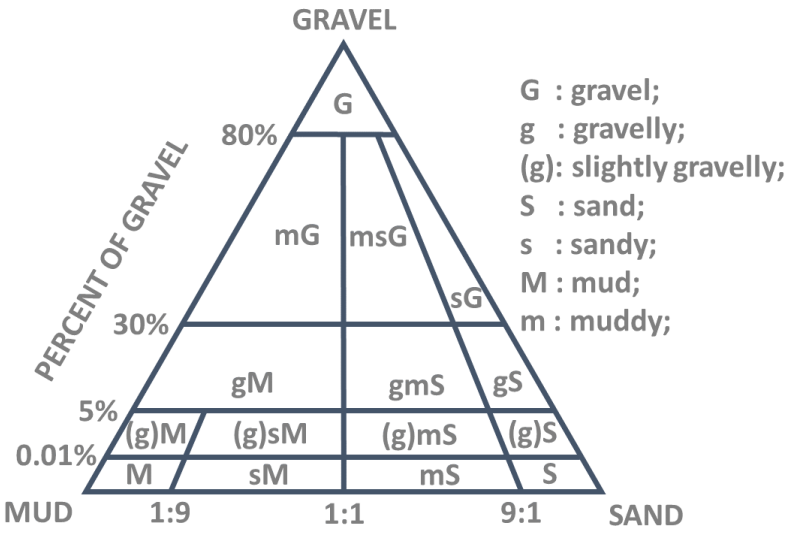

Figure 2.2: Sediment textural groups triangle, after Folk (1954)

.

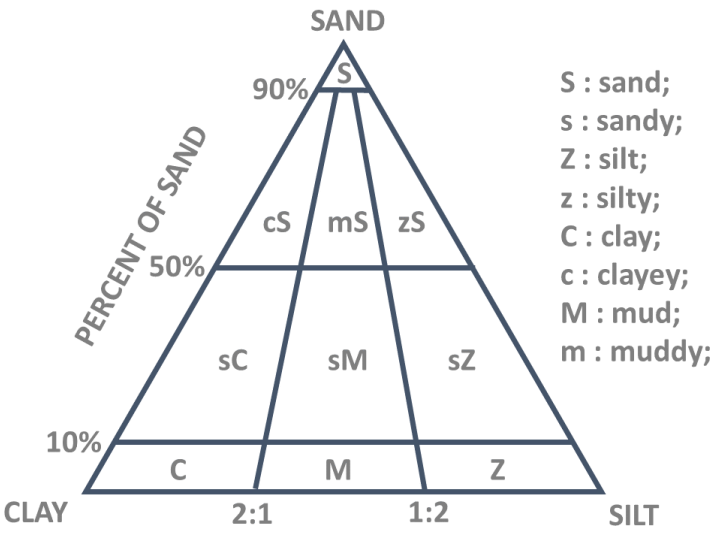

Figure 2.3: Sand-silt-clay textural groups triangle, after Folk (1954)

.

number of boulders and cobbles may detach from cliffs into the sea. However, sediment entrainment occurs at speeds that are not large enough, in general, to entrain boulders into the flow, and therefore we will not elaborate more into this idea of a gravel-cobble-boulder textural group triangle.

Sediment entrainment depends on the shear stress, τ, as introduced in Chapt. 1. The dimensionless shear stress, τ^*, also known as the Shields parameter, θ, may be expressed as

$$\tau^* = \theta = \frac{\tau}{(\rho_s - \rho)gD}, \tag{2.1}$$

where ρ_s is the density of the sediment; ρ the density of the fluid; g the acceleration due to gravity; and D the characteristic diameter of the particle, usually the median grain diameter, d_{50}. Physically, θ is proportional to the ratio of 1) the force applied by the fluid on the particle, and 2) the weight of the particle. When a particle is resting on the seabed, additional particle-to-particle contact forces maintain the sediment in an equilibrium position in relation to the bed. Closest to the particle surface, viscous shear stresses act on the boundary and the boundary layer flow field $U(z)$ follows, approximately, a viscous linear profile:

$$U(z) = \frac{u_*}{\delta_\nu} z, \tag{2.2}$$

where $\delta_\nu = \nu/u_*$ is the viscous length and u_* the friction velocity. Further away from the surface, the fluid forces produce a positive (upstream) and negative (downstream) pressure field around the particle. The sum

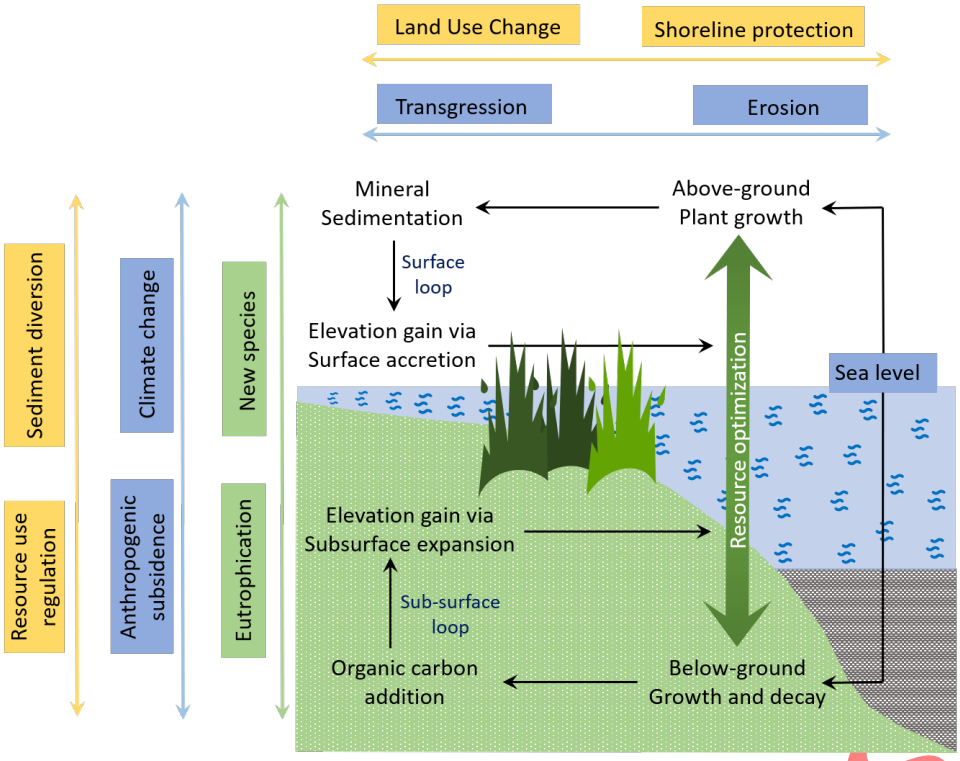

Figure 2.27: Schematic of wetland cycles and processes relevant for wetland evolution. Modified from Kirwan & Megonigal (2013).

changes in sea level. When the opposite holds, i.e., the bed elevation is lower that what is optimal for primary production, then the system is unstable. Morris et al. (2002) also identified an optimal rate of relative sea level rise (RSLR), for which the bed level changes and the depth of the tidal inundation are at equilibrium, and plant growth is optimal. Also, when the RSLR is above its optimal value, vegetation growth cannot sustain the necessary bed level increases that are necessary to maintain the equilibrium. Morris et al. (2002) and Temmerman et al. (2003) showed that the incoming suspended sediment concentrations affect wetland stability, with Temmerman et al. (2003) pointing out that saltmarsh erosion occurs with decreases of either the inundation depth or the incoming suspended sediment concentrations (SSC). So it is essential to consider both inundation and sediment renourishment sources in wetland morphodynamic modelling.

In a complementary study carried out by D'Alpaos et al. (2007), the authors analysed the effects of sediment transport, vegetation growth and sea level rise on the network of flooding and ebbing channels that characterize intertidal flat ontogeny D'Alpaos et al. (2005), and evolving landscapes. D'Alpaos et al. (2007) showed that marsh ecology is a crucial driver of long-term wetland morphological evolution. The authors showed that if the vegetation is dominated by one single species, namely by Spartina, then under constant

rates of sea level rise, unvegetated and Spartina-dominated environments tend to an equilibrium at or below Mean High Water Level (MHWL) under adequate sediment supply and vegetation growth conditions, but marshes with multiple vegetation species can make a transition upland. By tracking the growth of the intertidal platform, the evolving channel morphology and the vegetation dynamics, D'Alpaos et al. (2007) were able to analyse the mechanisms driving the sedimentation patterns observed in tidal environments, based on different suspended sediment concentrations, relative mean sea level rise conditions, and absence or presence of vegetation.

The last two models to discuss are those by Kirwan & Murray (2007) and Mudd et al. (2009). As D'Alpaos et al. (2007), Kirwan & Murray (2007) analysed landscape evolution and platform changes in wetland environments, through the coupling of geomorphic and ecological models. In addition to other factors mentioned by previous authors, Kirwan & Murray (2007) also considered the creek bank slumping and other slope-driven transport processes that are driven by vegetation biomass. They analysed different sea level rise scenarios, starting from a steady moderate rise, and increasing the rate of sea level rise. They showed that wetland vegetation can maintain the wetland environment in a metastable equilibrium, even under rapidly rising sea levels, demonstrating the importance of vegetation on wetland habitat conservation. Kirwan & Murray (2007) and Mudd et al. (2009) considered a model that can reproduce wetland platform and channel network evolution. Mudd et al. (2009) considered the above-ground and below-ground organic matter cycles - schematized in Fig. 2.27. For the above-ground organic production cycle, they defined the sediment deposition rate as a function of vegetation density, and horizontal distance from a channel, but did not include channel erosion. However, without erosion the impact of an expanding tidal prism on channel network erosion and expansion, for example, and the subsequent reduction in wetland area (Allen 1997), cannot be taken into account.

We conclude this section with a brief description of the wetland processes included in the model developed by Kirwan & Murray (2007). First, each model iteration is initiated with the high tide water level and the topography is partitioned into 5 m by 5 m cells. Then, the total draining volume of water per cell for a single ebb flow is computed. The water drains off of the marsh platform, through the channel network, and out of the basin according to flow directions defined by a parametrically represented water surface, without the need for intratidal velocity computations. The volume of water, V, that flows through a given cell is related to high-tide level, s, and the bed elevations, $z(x, y)$, of its watershed, w (Rinaldo et al. 1999):

$$V = \int_w [s - z]\, dxdy. \tag{2.66}$$

The maximum value of $s - z$ is limited by the tidal range, and so cells with elevations that are below low tide do not drain completely. The volume of water is computed over a characteristic time scale of three hours, to obtain the near-peak water discharge (19). The discharge must be divided by some water depth, to ensure that velocity is higher in shallower areas and lower in deeper areas, for a given discharge (Fagherazzi & Furbish 2001). Then the erosion rate is computed in terms of the bed shear stress, $\tau_b = \rho f_c U_*^2/8$, as

$$\text{Erosion rate} = \frac{m\,(\tau_b - \tau_c)}{\tau_c}, \tag{2.67}$$

where ρ is water density, $f_c = 0.02$ is a friction factor, U_* is the bottom friction speed, $m = 0.0014$ kg/m^2 per second, and $\tau_c = 0.4$ N/m^2 is the critical shear stress, defining the threshold of erosion (Fagherazzi & Furbish 2001). As most erosion occurs over intermittent, near-peak flows, which occur only once over the tidal cycle and have a duration of around 10 minutes. So the erosion rate is multiplied by 10 minutes to compute the erosion rate over a single tidal cycle. The model also includes formulations for the Deposition rate, the Biomass productivity, and the Slope-driven sediment transport. Finally, a number of experiments are carried out to model the evolution and dynamic equilibrium of the marsh channel-platform morphology; this dynamic equilibrium is reached when the elevation change everywhere equals the rate of sea-level rise, and the water depth remains constant. This simple model captures several wetland platform and channel network characteristics, for example the channels become wider downstream. Also, the platform morphology, water depth, and rates of biomass productivity agree well with observations.

Chapter 3

Modelling Procedures and Best Practices

3.1 Modelling concepts and methods for different scales and applications

The fundamental physics of estuaries and coastal environments were introduced in the last chapter. The formulations discussed were obtained through laboratory, field, and remote sensing observations, and provide an understanding of the evolution in space and time of sediment concentration fields, seabed heights and estuarine depths and widths, bottom shear stress formulations and sediment fluxes, amongst others. The dynamics of these environments may be analysed using dimensionless parameters: the Reynolds number, the Froude number, the Shields parameter, to name but a few. In the case of wave dynamics, some dimensionless parameters may be rather simple, such as the wave steepness, i.e. the wave height to wavelength ratio, or the relative water depth, i.e the water depth to wavelength ratio. As explained in Chapt. 2, dimensionless parameters are most useful because their size determines important physical characteristics of the system, in particular in limiting cases some terms in the equations of motion may be neglected and, importantly, this will lead to simplified equations that can be solved analytically. For example, the relative water depth is an essential parameter in wave dispersion processes, because it determines whether waves are dispersive or non-dispersive, and whether the wave height, length and celerity are influenced by water depth (Benassai 2006).

In any modelling effort, it is necessary to inspect the boundary and initial conditions that are most appropriate at the scales of interest. The boundary parameters and variables that need to be defined also depend on the type of boundary. In coastal area models, one needs to consider three types of boundaries. At the ocean or land-ocean boundaries, the incoming hydrodynamic conditions need to be defined, such as: waves, tides, storm surges, coastal inlet or estuarine discharges. At bottom boundaries, the bathymetry (a map of the seabed) or the *topobathy* (a map combining topography and bathymetry), the bottom characteristics and associated model parameters, such as the bottom roughness, need to be considered (Van Dongeren et al. 2013, Kono et al. (in prep.)). And finally, at atmosphere-ocean (either oceanic or estuarine) boundaries, water surface pressures, heat fluxes, and wind shear stresses need to be analysed. In biogeochemical and water quality problems, one may include, additionally, advection-diffusion-reaction-decay equations for sediments, pollutants and nutrients. In other applications, one may also need to consider chemical transfer equations between the water and the atmosphere. Passive tracers can be analysed following dispersion concepts, thus avoiding the complexities associated with chemical or biological activity; such approach is valid, for example, for fish larvae dispersion in upwelling regions.

Therefore, generally in morphodynamic models we will need to define the following forcing parameters (Roelvink & Reniers 2012): the tidal characteristics (amplitude or phase) over a spring-neap cycle; the offshore wave conditions at a representative location, or at several locations along a model boundary - significant wave height, period and direction, as well as the wave energy spectral shape; sea surface wind speed and direction, and sea level pressure when available; river discharges (and constituent characteristics, when relevant); and surge level during extreme event conditions. As Roelvink & Reniers (2011) point out, care must be taken with correlated parameters. For example, the surge level is often correlated (with lots of scatter) to the wind, and (for a given direction) to the waves; the locally generated wave direction is correlated with the wind direction, especially under strong winds; the locally generated wave heights and wind speeds are correlated, for a given direction; and the locally-generated wave period is correlated with the wave height. The tidal boundary conditions are uncorrelated with other forcings, although tides may be modified by surges, winds, and waves.

3.1.1 Mesh generation

3.1.1.1 Mesh design in the horizontal coordinates

Designing a good quality mesh, whether it is a spherical or a topologically Cartesian one, is an essential consideration in the model design process, in particular around the area of interest. Several modelling suites

have their mesh generator, which facilitates and speeds up the process. In this section we will use numerical tide and storm surge modelling examples. Numerical storm surge modelling and prediction intensified in the countries bordering the North Sea after the great storm surge of 31 January to 2 of February 1953, which caused severe coastal damage in The Netherlands, the UK, and Germany. Due to this storm, coastal management policies changed significantly in these countries. Extreme event modelling is obviously important for a number of reasons, as pointed out by Flather (1984). Firstly, such events may cause severe damage and loss of lives around the world, and therefore any forecasting model needs to be able to reproduce the impacts of such events. Secondly, numerical models give spatio-temporal information on storm surge evolution that is generally impossible to obtain by other means. Finally, the numerical model predictions of surge and tidal water levels can be used for coastal defence design.

We will first discuss the grid generation options on the horizontal coordinates, or the latitude and longitude coordinates in large geographical domains. Along these two coordinates, the models may use regular Cartesian grids, regular curvilinear grids, unstructured meshes, or a combination of those. Regular Cartesian grids were common in early modelling efforts, for example in numerical storm surge modelling by Hansen (1956, cited by Flather 1984) and (Prandle & Wolf 1978). Due to their relevance and simplicity they are still used in current applications. Cartesian grids may be have uniform, non-uniform ('plaid') or adaptive grid spacing (van Hooft et al. 2018), and may be locally refined, as in quadtree models (Popinet & Rickard 2007). Two methods are available for local grid refinement, namely: domain decomposition (Funaro et al. 1988) and nesting methods (Cailleau et al. 2008). They both are implemented in a number of ocean and coastal hydrodynamics models, such as in the Dutch codes TRISULA (currently known as Delft3D-FLOW) or SIMONA, both for Cartesian and for regular curvilinear grids (de Goede et al. 1995). Figure 3.1 shows a close-up of a Cartesian grid (Fig. 3.1a) and a curvilinear grid (Fig. 3.1b), for a coastal region in the Upper Gulf of California, around San Jorge Island, which is in fact an archipelago of smaller islands. The largest island is very long, with a length of around one kilometre, and very narrow, with a width of around 185 m at its widest location. Its northern beach (the only beach), used by the seal colony, is geographically located at (31° 00' 59.47" N, 113° 14' 42.22" W).

Curvilinear grids evolved from Cartesian meshes as a more advanced level of complexity (Amsden & Hirt 1973), even if curvilinear grids are topologically equivalent to Cartesian grids. A curvilinear grid has important advantages in comparison to a Cartesian grid, as by design the grid can adjust to offshore structures, or follow coastlines or isobaths. Like Cartesian grids, curvilinear grids are structured meshes, except they may not be orthogonal. However, some orthogonality conditions usually are necessary, for code robustness and

3.4 Data-driven modelling

Data-driven modelling is an interdisciplinary field of science, that focuses on statistical and pattern analysis of observations or model outputs. Data-driven methods may be divided into linear (Larson et al. 2003), and non-linear techniques (Southgate et al. 2003). Examples of linear methods include bulk linear statistical methods, Principal Component Analysis (PCA) and any variation of PCA, Canonical Correlation Analysis (CCA), Empirical Orthogonal Teleconnections (EOT), or statistical clustering. Examples of non-linear methods include extended EOF (EEOF), Singular Spectrum Analysis (SSA), Fractal analysis, Wavelet Analysis, or Neural Networks. Some of these methods are described in more detail in this section, based on case study examples collected from the literature. Recent research has combined data-driven schemes with numerical models (Alvarez & Pan 2016) or with reduced-complexity approaches (Reeve et al. 2016), to extract coastal patterns and analyse their spatio-temporal behaviour. Empirical Orthogonal Function (EOF) methods were first applied to beach morphodynamics by Winant et al. (1975), who used monthly beach data from Torrey Pines Beach, California, collected over a period of two years. They found that most of the beach variability could be explained by the first three principal components, which corresponded, physically, to the mean beach profile, the onshore-offshore seasonal bar migration, and the low-tide terrace. This pioneering work with EOFs has been followed by several studies on, for example, barrier islands (Aranuvachapun & Johnson 1978), beach level variability through beach profile time sequences (Wijnberg & Terwindt 1995), sandbank and coastal channel evolution (Reeve et al. 2008). Let ξ_l be the spatial coordinate and t_k the temporal coordinate, and the bed level be defined as $g(\xi_l, t_k)$, with $1 \leq l \leq L$, $1 \leq k \leq K$. Note that any spatially two-dimensional data can be expressed with one spatial coordinate, by reorganizing the M-by-N matrix into a column vector with dimensions MN-by-1. EOF and PCA rely on the separation of the signal into spatial and temporal variabilities, so conceptually the goal of the method is to separate the signal as

$$g(\xi_l, t_k) = \sum_{p=1}^{L} \alpha_p c_p(t_k) e_p(\xi_l), \tag{3.43}$$

The normalization factors depend on the dimensions of the domain, $\alpha_p = \sqrt{\lambda_p LK}$, and the functions e_p, the spatial eigenfunctions, with their corresponding the eigenvalues λ_p, are determined directly as the eigenfunctions of the square $L \times L$ correlation matrix of the data, $\mathbf{A}$,

$$\mathbf{A} e_p = \lambda_p e_p, \tag{3.44}$$

Note here that is **A** is real and symmetric it has L real eigenvalues, and its eigenvectors may be chosen as mutually orthonormal, that is,

$$\sum_{l=1}^{L} e_p(\xi_l)e_q(\xi_l) = \delta_{pq} \tag{3.45}$$

where δ_{pq} is the Kronecker delta. The correlation matrix is calculated directly from the data. It has $L \times L$ elements a_{mn} of the form:

$$a_{mn} = \sum_{K}^{k=1} \frac{1}{LK} g(\xi_n, t_k)g(\xi_m, t_k), \text{with} 1 \leq \text{m, n} \leq \text{L} \tag{3.46}$$

The functions $c_p(t_k)$, the temporal eigenfunctions, satisfy:

$$c_p(t_k) = \sum_{p=1}^{L} g(\xi_l, t_k)e_p(\xi_l), \tag{3.47}$$

with the normalization factors now incorporated in c_p. From the properties of real symmetric matrices one can deduce one can deduce some of the properties of the properties of the data:

- The trace of **A** is equal to the mean-square value of the data, or the energy;
- Each eigenvalue λ_p, represents the relative contribution of mode p to the total variability;
- The matrix can be arranged so that λ_i are in decreasing order with increasing i, so that e_1 accounts for most of the mean-square value, e_2 for most of the remaining mean-square value, and so on;
- In general, the first five modes capture more than 90% of the total energy, unless the system has a lot of red noise (Vautard & Ghil 1989);
- The shape functions can be interpreted as "modes" of variation, as in Fourier analysis; and
- The number of maxima and minima in an eigenfunction increases with the order of the eigenfunction.

In the analysis above we have only considered one spatial variable ξ_l, but a two-dimensional space (x_i, y_i) can always be mapped onto a one-dimensional array ξ_l, with a book-keeping method that helps arrange the eigenfunctions back into the original two-dimensional space, and plot them easily into contour maps for the interpretation of results. The dynamics that can be resolved with data-driven methods will depend very strongly on the spatial and temporal resolution of the data. It is essential to take those limitations into account, from the moment the research is being planned. For example, in Reeve et al. (2008), the spatio-temporal resolution of the bathymetric data is sufficient to analyse the sandbank and channel evolution, but

not detailed enough to analyse the dynamics of ripples. In fact, due to the characteristics of coastal areas it is often difficult to obtain appropriate datasets in order to apply the EOF method intensively. However, some data acquisition techniques, such as video cameras or satellite imagery, can help with the acquisition of beach data that lends itself well to the application of the EOF method (Fairley et al. 2009). EOF components allow describing changes occurring over the period covered by the data. However, EOF can be combined with different extrapolation techniques, in order to quantitatively assess the data variability beyond the observation period. However, as in Reeve et al. (2008), in most cases the extrapolation is limited to the EOF temporal component.

While EOF analysis is one of the most widely used linear data-driven methods, its non-linear counterpart, the extended EOF (EEOF) analysis or Singular Spectrum Analysis (SSA), is less popular for beach data. However, it has been used to assess sandbar variability in the Baltic Sea (Różyński et al. 2001), and to analyse long-term trends in shoreline position at several beaches around the world (Southgate et al. 2003, Różyński 2005). SSA, which is described in detail by (Elsner & Tsonis 1996), has been applied extensively to several oceanographic and meteorological time series (Ghil 2002). As with all data-driven techniques, SSA separates the data into a trend, some oscillatory components that can explain periodicity patterns at different time scales, and noise. With the multivariate version of SSA, the MSSA, the data matrix may include not only the bathymetry but also the forcing data. MSSA was applied, for example, to monthly time series of beach elevations, water levels, wave heights, and sea level pressure differences associated to the North Atlantic Oscillation at Duck, North Carolina, to assess monthly to yearly sandbar migration cycles and the possible forcing mechanisms of such cycles (Magar et al. 2012).

Finally, current research has focused on the development of hybrid data-driven methods, or on data-driven methods applied to numerical model outputs. Data-driven methods have also benefited in recent years from the availability of high quality remote sensing imagery from satellites, the widespread use of stationary beach cameras, or imagery from drones. These data sources are more valuable when combined with in-situ monitoring of the forcings driving coastal change, such as waves, tides, river discharges, and storm surges. Reeve et al. (2016) argue that successful solutions will need to account for cause-effect dependencies, between forcings and beach change observations, which can explain morphological tendencies and patterns at time scales of 10 to 100 years, and length scales of 10 to 100 kilometres.

Chapter 4

Future Modelling Applications

4.1 Climate Change - Storm Surge and Inundation Modelling

Here a climate change impact assessment is presented, together with an adaptation good practice (AGP) numerical modelling case study, developed for Bunbury, a small city in South Western Australia. The methodology is explained in detail by Fountain et al. (2010), and the aspects that are most relevant for regional modelling are summarized in this section. The purpose of the study was to develop a methodology with open source software, that could be understood and implemented very easily by coastal authorities. The information published by the Australian National Climate Change Adaptation Research Facility (NCCARF) is publicly available – see www.nccarf.edu.au (NCCARF 2014), for this case study and for additional examples. The Bunbury case study is an example of coupled modelling applied to coastal inundation under different sea level rise scenarios, combined with worst case storm tracks. The approach adopted involved integrating the outputs from Global Environmental Modelling Systems (GEMS) 2D Coastal Ocean Model (GCOM2D) regional scale storm surge model with the free and open source hydrodynamic modelling software ANUGA, to estimate inundation at the City of Bunbury resulting from a range of possible storms surge events. These models are used in conjunction with a Shoreface Translation Model (STM). The purpose of the study was to inform coastal practitioners and decision makers of the potential damage to coastal infrastructure under extreme events. For such studies to fulfil this purpose, it is necessary not only to analyse likely future climate trends, but also key climate change vulnerabilities, and different adaptation choices, not only to overcome barriers and minimize costs, but also to identify, pursue, and fund priority research.

The methodology couples three component models that have been validated independently. So, one of the aims was to validate the coupled modelling approach. The three components consist of two hydrodynamic models that work best at different scales: the storm surge model GCOM2D, or GEMS (Global Environmental Modelling Systems Pty Ltd) 2D Coastal Ocean Model (Hubbert et al. 1990, Hubbert & McInnes 1999); the open source, hydrodynamic and hydraulic ANUGA model (see https://anuga.anu.edu.au/), developed by Zoppou & Roberts (1999) and initially released to the Open Source community in 2006 through SVN by Geoscience Australia; and the Shoreface Translation Model (STM), developed by Cowell et al. (1992) at the University of Sydney. The model outputs may serve different purposes, for example, they may:

- Highlight the coastline areas that are most vulnerable to inundation;
- Raise community awareness to coastal risks and coastal protection;
- Inform town development policies, based on the risk of storm surge inundation; or
- Develop emergency planning responses and flood protection infrastructure.

4.1.1 Storm surge model GCOM2D

GCOM2D solves the shallow water momentum conservation equations in two (horizontal) dimensions. The model is driven by wind stress, atmospheric pressure gradients, astronomical tides and quadratic bottom friction (Hubbert et al. 1990). At the air-sea interface, an atmospheric forcing derived from the lowest level of a limited-area, numerical weather prediction model is applied (Leslie et al. 1985), but with variations on surface roughness and with atmospheric instability taken into account through a boundary-layer model. The non-linear momentum conservation equations solved by GCOM2D are as follows:

$$\frac{\partial U}{\partial t} - fV = -mg\frac{\partial \eta}{\partial x} - \frac{m}{\rho_w}\frac{\partial P}{\partial x} - m\left(U\frac{\partial U}{\partial x} + V\frac{\partial U}{\partial y}\right) + \frac{1}{\rho_w H}\left(\tau_{sx} - \tau_{bx}\right) \quad (4.1)$$

$$\frac{\partial V}{\partial t} + fU = -mg\frac{\partial \eta}{\partial y} - \frac{m}{\rho_w}\frac{\partial P}{\partial y} - m\left(U\frac{\partial V}{\partial x} + V\frac{\partial V}{\partial y}\right) + \frac{1}{\rho_w H}\left(\tau_{sy} - \tau_{by}\right), \quad (4.2)$$

where the chosen map projection is taken into account explicitly through a map factor m, and x and y are the horizontal Cartesian coordinates in the map projection's plane. Here (U, V) are the depth-integrated current velocity components, η is the free surface elevation, H is the total water depth, f the Coriolis parameter, P the atmospheric sea surface pressure, $\vec{\tau}_s = (\tau_{sx}, \tau_{sy})$ the sea surface wind stress, and $\vec{\tau}_b = (\tau_{bx}, \tau_{by})$ the

bottom shear stress. The continuity equation is of the form

$$\frac{\partial \eta}{\partial t} = -m^2 \left\{ \frac{\partial}{\partial x}\left(\frac{UH}{m}\right) + \frac{\partial}{\partial y}\left(\frac{VH}{m}\right) \right\}. \tag{4.3}$$

The surface wind stress and the bottom shear stresses are both determined using quadratic relationships. In the case of $\vec{\tau}_s$, we have

$$\tau_{sx} = C_D \rho_a \left(U_{10}^2 + V_{10}^2\right)^{1/2} U_{10}, \text{and} \tag{4.4}$$

$$\tau_{sy} = C_D \rho_a \left(U_{10}^2 + V_{10}^2\right)^{1/2} V_{10}, \tag{4.5}$$

where (U_{10}, V_{10}) are the wind velocity components 10 m above sea level, ρ_a is the air density, and C_D is the sea surface drag coefficient. A number of formulations for C_D exist in the literature. For GCOM2D, Hubbert et al. (1990) apply the definitions adopted by Smith & Banke (1975), where C_D depends on a wind speed threshold. Below wind speeds of 25 m/s, C_D is defined as

$$C_D = \left[0.63 + 0.066 \left(U_{10}^2 + V_{10}^2\right)^{1/2}\right] \times 10^{-3}, \tag{4.6}$$

and above wind speeds of 25 m/s, the expression for C_D becomes

$$C_D = \left\{2.28 + 0.033 \left[\left(U_{10}^2 + V_{10}^2\right)^{1/2} - 25.0\right]\right\} \times 10^{-3}. \tag{4.7}$$

The bottom shear shear stress, on the other hand, is proportional to the current velocity,

$$\vec{\tau}_b = K \rho_w \left(U^2 + V^2\right)^{1/2} \vec{U}, \tag{4.8}$$

with $K = 2 \times 10^{-3}$ or 2.5×10^{-3}, depending on the model calibration (Hubbert et al. 1990, Flather 1984). Other bottom friction coefficient formulations, for example that of Mofjeld (1988), suggest that K should depend on the ratio H/z_0, where z_0 is the bottom roughness, which corresponds to the height above the seabed at which the no-slip condition is applied. In GCOM2D, K is a constant and is set to 2×10^{-3}.

The boundary and initial conditions are as follows. The normal component of the velocity vanishes at coastal boundaries. At open boundaries, the component of the current along the outward directed normal (U_n) depends on the water depth, the sea surface elevation, and the phase speed, $C_p = \sqrt{gH}$, of shallow-water

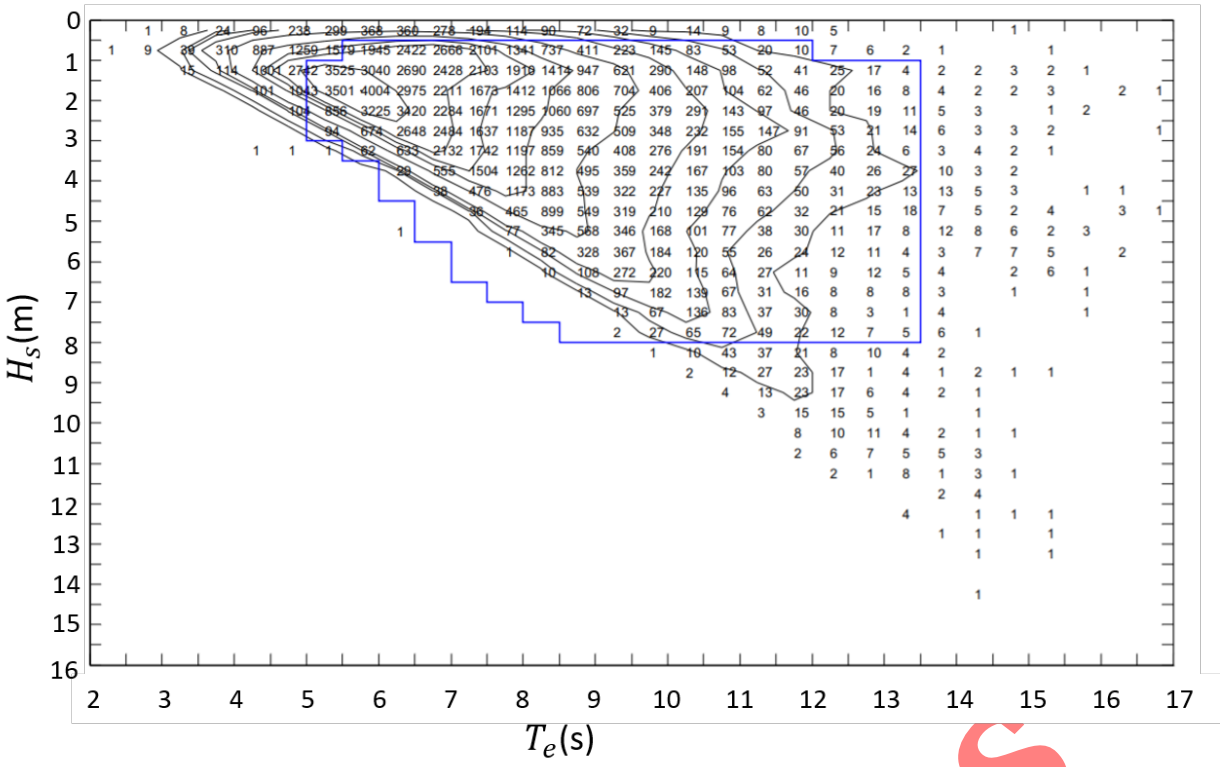

Figure 4.21: $H_s - T_e$ diagram for Wave Hub Site using wave conditions from a 40-year simulation with WW3. From Reeve et al. (2011).

first half of 2019 (Web of Science 2019). However, within this broad research topic, only 476 papers have focused on environmental impacts, with three universities accumulating 50 research products: the Norwegian University of Science and Technology NTNU (24), the University of Plymouth (14), and Delft University of Technology (12). Most of these outputs are the result of a number of projects that have been approved by either National or EU research councils. For example, during her time at the University of Plymouth, and later at CICESE, the author participated in the INTERREG project "Offshore Foundations' Environmental Impact Assessment" (OFELIA) – see https://www.keep.eu/project/7983/ofelia for more details. This project focussed on hydrodynamic and sediment transport impacts of offshore wind turbine monopile foundations. In particular, several physical modelling studies at laboratory scales where carried out in all three partner universities (University of Caen, University of Le Havre, and University of Plymouth). A numerical modelling exercise at regional scales was also performed, using the Courseulles-sur-Mer wind farm site as case study (Rivier et al. 2016).

The regional hydrodynamic model used in OFELIA was the MARS3D model of IFREMER, developed by Lazure & Dumas (2008). MARS3D is applicable to coastal bays and estuaries, with a coupling be-

tween barotropic and baroclinic modes which allows for consistent sediment and pollutant transport between the 2D and the 3D configuration of the model. Like Delft3D, MARS3D is by default a terrain-following model, with vertical layers corresponding to normalized isopycnal layers of constant density, as introduced by Phillips (1957) and Bleck & Smith (1990). The depth normalization helps maintain high resolution in the model in a wide range of water depths. Some shallow-water models use a time splitting scheme that solves implicitly the internal waves (the internal mode) with large timesteps, and explicitly the free surface (gravity) waves (the external mode) with small timesteps. The two modes have a two-way coupling: the barotropic pressure gradient is prescribed by the external to the internal mode; and bottom stress, integrated pressure gradient and internal stresses are provided by the internal to the external mode (Lazure & Dumas 2008). However, other models have been adapted and they can us an implicit or semi-implicit numerical scheme to solve the equations for the external, barotropic mode; in this case, the internal and external modes can be solved with large timesteps, as the CFL stability conditions is removed. MARS3D uses an Alternative Direction Implicit (ADI) scheme (Lazure & Dumas 2008), and thus falls into this latter category.

The sediment transport module in MARS3D is based on the advection-diffusion equation formulated by Hir et al. (2011), with a bottom boundary condition involving erosion and deposition processes which are adequate for sand and mud mixtures. In Rivier et al. (2016) the sediment fluxes, deposition and erosion rates, and settling velocity was determined using a current flume experiment set-up, where the sediment grain sizes varied between 140 and 450 μm. They only considered the suspended sediment concentration, with a fixed bedlevel in the hydrodynamic module, but a variable spatio-temporal availability of sediments inducing a change of bed thickness in the sediment transport module. The original contribution of Rivier et al. (2016) consists on the implementation in MARS3D of a drag force, $\mathbf{F}_D$, per unit area induced by the monopile, defined as

$$\mathbf{F}_D = -\frac{1}{2}\frac{\rho_w C_D D}{\Delta x \Delta y} \parallel \mathbf{u}_\infty \parallel \mathbf{u}_\infty \tag{4.14}$$

where ρ_w is the water density; C_D is the drag coefficient; D is the monopile diameter; Δx and Δy the cell sizes in the x and y directions, respectively; $\parallel \cdot \parallel$ is the L^2 norm; and $\mathbf{u}_\infty$ (u_∞, v_∞) is the undisturbed current velocity upstream of the pile. The drag force terms are added to the conservation and the turbulence closure equations of the model. The effects of the monopile on the hydrodynamics and the sediment transport are evaluated using the relative difference

$$\Delta V = \frac{V_{mod} - V_{ref}}{V_{ref}}, \tag{4.15}$$

for each variable V of interest, with V_{mod} the values with the monopile, and V_{ref} the reference (undisturbed

flow) values. The impact of the monopiles was evaluated using the new implementation and the default, dry cell approach already available with MARS3D. Two monopile diameters, of 6 m and 15 m, were also analysed. In the first case, the monopile covers 4 cells and appears as a square in an $x - y$ plane, whereas in the second one the monopile covers 21 cells. The analyses was based on four monopiles forming a square, with a side of 950 m.

The main conclusions of Rivier et al. (2016) were the following:

- currents accelerate on the upstream side of the monopile, and decelerate on the downstream side.
- In the regions with larger current speed and shear stress, erosion and sediment re-suspension is observed.
- Sediment deposition occurs in regions with weak bottom shear stress, as expected.
- If a monopile wake reaches another monopile, then it will affect the hydrodynamics and sediment transport in the vicinity of that monopile too.

The conclusions above are obtained with both the code with drag forces and the code with dry cells at the position of the monopiles. The main difference between the two methods is that, Erosion and deposition are higher close to the monopile with the parameterization method than with the dry points method. For both approaches, the monopile wake can be observed even 2 kilometres downstream of the monopile, and thus it will affect other monopiles in the array if they are in the wave path.

Chapter 5

Epilogue

Our journey has come to an end. In these pages, we attempted to provide comprehensive coverage of sediment transport and morphodynamic modelling for coasts and shallow environments, with an emphasis on the physical processes, the modelling design, and the more significant results, at different dynamic scales.

We started describing the dynamics of the coastal environment from the microscopic to the macroscopic scales, possibly because it was more intuitive to do it like so. We also strived to describe in detailed the physical processes first, and then see how the physics are implemented in numerical models.

In the fundamental physics chapter, we start with sediment composition concepts and move on to sediment transport formulations, with descriptions of the flow characteristics in the bottom boundary layer. We then analyse the processes responsible for sediment transport, both in the deep ocean and in coastal waters, with a focus on the effects of waves and tides on sediment transport and morphodynamics. We evaluate in detail the roles that waves and tides play in the evolution of open coasts and sheltered coastal ecosystems. We also assess the differences in sediment composition and vegetation type and coverage between these two contrasting coastal environments.

In the numerical modelling chapter, we place significant emphasis on good modelling practices, particularly for shallow water regional models. However, these practices apply to other model types, such as Reynolds-Averaged Navier-Stokes (RANS), Large-Eddy Simulation (LES), or Direct Numerical Simulation (DNS) models. We start with mesh development issues, such as a presentation on structured and unstructured grids, suggestions on grid resolution needs according to the study objectives, and properties of sigma-level and z-level meshes. We then comment on different bathymetries of global coverage available online, as well

as high-resolution bathymetries obtained with in-situ and remote sensing measurements. A discussion on tidal, wave and meteorological forcings follows, together with a description of different models that couple hydrodynamics, sediment transport, and morphodynamics. We close this chapter with some case studies on numerical modelling for complex environments. The final chapter contained a series of examples that illustrate novel and future applications of morphodynamic modelling. These examples focus principally on:

- the evaluation of potential climate change impacts on the coast and climate change mitigation strategies,
- new coastal mega beach nourishment projects that reduce the need for regular interventions and thus reduce the costs of coastal protection, and
- studies on potential environmental impacts of offshore renewable energy farms.

We would have liked to have been able to expand more on several modelling approaches, that unfortunately we only covered superficially. Such is the case, for instance, for Boussinesq-type models. The effects of meteorological forcings on the evolution of complex environments should also expand in future editions. We engaged, mostly, on the description of regional models forced by tides and by spectral wave formulations. Not because they are the best models, but because they are used extensively in industry, and they provide useful insights into the short to medium-term evolution of coastal environments. Another possible weakness remains in the presentation of the most significant results concerning previous research. However, I hope to have corrected this in most cases.

Climate change will have predicted and unforeseen impacts on coastal environments. Therefore, as coastal modellers, it is our responsibility to envision different scenarios and assess the effects of extreme events on coastal ecosystems and urbanized coasts alike. While the economic costs of damage to coastal cities are evident, coastal ecosystems provide vital services to humankind. Offshore reefs, for example, protect the coast from erosion by incoming storms through dissipation of wave energy. Mangroves and saltmarshes also dissipate wave energy, and at the same time act as sediment traps. Sea level rise will force us more and more to design managed realignment schemes, to reduce the costs associated with the protection of our assets.

In the 20th-century humankind tended to use hard engineering structures for coastal protection, which led to the loss of whole coastal towns, due to a lack of detailed understanding of the sediment pathways. However, we seem to have realized that working with nature will provide better long-term solutions to coastal erosion and flooding. 21st-century coastal protection designs are a reflection of this new philosophy. This is evident, for example, in the case of the floating gardens and play areas designed to protect the coastal sectors of New York City.

Finally, we concluded with environmental impacts of offshore structures, in particular offshore renewable energy devices, and with a focus on devices that extract kinetic energy such as wave energy converters, wind energy farms, and in-stream tidal energy converters. We analysed some of their effects on nearby bedforms and coastlines, which are still poorly understood. A topic that is still missing here, is the greenhouse gas storage capacity of saltmashes, mangroves, and other coastal environments. We will attempt to include examples of human interventions that have, or could, promote this storage capacity through managed realignment schemes, in subsequent edition of this work.

Bibliography

Abanades, J., Greaves, D. & Iglesias, G. (2014), 'Coastal defence through wave farms', *Coastal Engineering* **91**, 299–307.
URL: *https://doi.org/10.1016/j.coastaleng.2014.06.009*

Achete, F., der Wegen, M. V., Roelvink, J. A. & Jaffe, B. (2017), 'How can climate change and engineered water conveyance affect sediment dynamics in the san francisco bay-delta system?', *Climatic Change* **142**(3-4), 375–389.
URL: *https://doi.org/10.1007/s10584-017-1954-8*

Ahmadian, R., Falconer, R. & Bockelmann-Evans, B. (2012), 'Far-field modelling of the hydro-environmental impact of tidal stream turbines', *Renewable Energy* **38**(1), 107–116.
URL: *https://doi.org/10.1016/j.renene.2011.07.005*

Alexander, K. S., Ryan, A. & Measham, T. G. (2012), 'Managed retreat of coastal communities: understanding responses to projected sea level rise', *Journal of Environmental Planning and Management* **55**(4), 409–433.
URL: *https://doi.org/10.1080/09640568.2011.604193*

Allen, J. (1997), 'Simulation models of salt-marsh morphodynamics: some implications for high-intertidal sediment couplets related to sea-level change', *Sedimentary Geology* **113**(3), 211 – 223.
URL: *http://www.sciencedirect.com/science/article/pii/S0037073897001012*

Alvarez, F. & Pan, S. (2016), 'Predicting coastal morphological changes with empirical orthogonal function method', *Water Science and Engineering* **9**(1), 14–20.
URL: *https://doi.org/10.1016/j.wse.2015.10.003*
ΩÁlvarez et al.

Álvarez, L. G., Suárez-Vidal, F., Mendoza-Borunda, R. & González-Escobar, M. (2009), 'Bathymetry and active geological structures in the Upper Gulf of California', *Boletín de la Sociedad Geológica Mexicana* **61**(1), 129–141.

Amsden, A. & Hirt, C. (1973), 'A simple scheme for generating general curvilinear grids', *Journal of Computational Physics* **11**(3), 348 – 359.
URL: *http://www.sciencedirect.com/science/article/pii/0021999173900788*

Andreotti, B. (2004), 'A two-species model of aeolian sand transport', *Journal of Fluid Mechanics* **510**, 47–70.

Andrews, D. G. & Mcintyre, M. E. (1978), 'An exact theory of nonlinear waves on a lagrangian-mean flow', *Journal of Fluid Mechanics* **89**(4), 609–646.
URL: *https://doi.org/10.1017/s0022112078002773*

António, S. D. (2017), Shoreline and sandbar coupling on a natural and nourished beach, Master's thesis, Department of Physical Geography,, Faculty of Geosciences, Utrecht University.

Aranuvachapun, S. & Johnson, J. A. (1978), 'Beach profiles at Gorleston and Great Yarmouth', *Coastal Engineering* **2**, 201–213.
URL: *https://doi.org/10.1016/0378-3839(78)90020-0*

Atkinson, A. L., Baldock, T. E., Birrien, F., Callaghan, D. P., Nielsen, P., Beuzen, T., Turner, I. L., Blenkinsopp, C. E. & Ranasinghe, R. (2018), 'Laboratory investigation of the bruun rule and beach response to sea level rise', *Coastal Engineering* **136**, 183–202.
URL: *https://doi.org/10.1016/j.coastaleng.2018.03.003*

Bagnold, R. A. (1966), An approach to the sediment transport problem from general physics, Technical Report 422–1, U.S. Geological Survey. Available at: https://pubs.usgs.gov/pp/0422i/report.pdf.

Balaji, R., Kumar, S. S. & Misra, A. (2017), 'Understanding the effects of seawall construction using a combination of analytical modelling and remote sensing techniques: Case study of fansa, gujarat, india', *The International Journal of Ocean and Climate Systems* **8**(3), 153–160.
URL: *https://doi.org/10.1177/1759313117712180*

Barnard, P. L., Schoellhamer, D. H., Jaffe, B. E. & McKee, L. J. (2013), 'Sediment transport in the san francisco bay coastal system: An overview', *Marine Geology* **345**, 3–17.
URL: *https://doi.org/10.1016/j.margeo.2013.04.005*

Barnard, P. L., Short, A. D., Harley, M. D., Splinter, K. D., Vitousek, S., Turner, I. L., Allan, J., Banno, M., Bryan, K. R., Doria, A., Hansen, J. E., Kato, S., Kuriyama, Y., Randall-Goodwin, E., Ruggiero, P., Walker, I. J. & Heathfield, D. K. (2015), 'Coastal vulnerability across the Pacific dominated by El Niño/Southern Oscillation', *Nature Geoscience* .

Bartholdy, J., Ernstsen, V., Flemming, B., Winter, C. & Bartholomä, A. (2008), On the development of a bedform migration model, *in* D. Parsons, T. Garlan & J. Best, eds, 'Proceedings of Marine and River Dune Dynamics III', University of Leeds, UK, pp. 9–16.

Battaglia, L., Cruchaga, M., Storti, M., D'Elía, J., Aedo, J. N. & Reinoso, R. (2018), 'Numerical modelling of 3d sloshing experiments in rectangular tanks', *Applied Mathematical Modelling* **59**, 357–378.
URL: *https://doi.org/10.1016/j.apm.2018.01.033*

Battjes, J. A. (1974), Computation of Set-up, Longshore Currents, Run-up and Overtopping due to Wind-generated Waves, Ph.D. thesis, Dept. of Civil Engineering, Delft University, Delft, The Netherlands. 241 pp.

Benassai, G. (2006), *Introduction to Coastal Dynamics and Shoreline Protection*, WIT Press, Southampton: UK.

Benoit, M., Marcos, F. & Becq, F. (2001), 'Development of a third generation shallow-water wave model with unstructured spatial meshing', *Coastal Engineering Proceedings* **1**(25).
URL: *https://icce-ojs-tamu.tdl.org/icce/index.php/icce/article/view/5241*

Berberović, E., van Hinsberg, N. P., Jakirlić, S., Roisman, I. V. & Tropea, C. (2009), 'Drop impact onto a liquid layer of finite thickness: Dynamics of the cavity evolution', *Physical Review E* **79**(3).
URL: *https://doi.org/10.1103/physreve.79.036306*

Bever, A. J. & MacWilliams, M. L. (2013), 'Simulating sediment transport processes in san pablo bay using coupled hydrodynamic, wave, and sediment transport models', *Marine Geology* **345**, 235–253.
URL: *https://doi.org/10.1016/j.margeo.2013.06.012*

Bird, E. & Lewis, N. (2015), *Beach Renourishment*, Springer International Publishing.
URL: *https://doi.org/10.1007/978-3-319-09728-2*

van Maren, D. S. (2009), 'Background theory cohesive-fine sediment-mud'. Last accessed on: 2018-03-25.
URL: *http://oss.deltares.nl/web/delft3d/community-wiki*

van Maren, D. & Winterwerp, J. (2013), 'The role of flow asymmetry and mud properties on tidal flat sedimentation', *Continental Shelf Research* **60**, S71 – S84. Hydrodynamics and sedimentation on mesotidal sand- and mudflats.
URL: *http://www.sciencedirect.com/science/article/pii/S0278434312001951*

van Rijn, L. C. (1993), *Principles of Sediment Transport in Rivers Estuaries and Coastal Seas.*, Aqua Publications, pp. 1.1–2.1.

van Rijn, L. C. (2007), 'Unified view of sediment transport by currents and waves. i: Initiation of motion, bed roughness, and bed-load transport', *Journal of Hydraulic Engineering* **133**(6), 649–667.
URL: *https://doi.org/10.1061/(asce)0733-9429(2007)133:6(649)*

van Rijn, L. C., Walstra, D. J. R. & van Ormondt, M. (2004), Description of transpor 2004 (tr2004) and implementation in DELFT3D-online, Technical Report Z3748, Delft Hydraulics, Delft, The Netherlands.

Van Rijn, L., Soulsby, R., Hoekstra, P. & Davies, A. G., eds (2005), *SANDPIT: Sand Transport and Morphology of Offshore Sand Mining Pits. Process knowledge and guidelines for coastal management. End document May 2005, EC Framework V Project No. EVK3-2001-00056*, Aqua Publications, The Netherlands.

Vautard, R. & Ghil, M. (1989), 'Singular spectrum analysis in nonlinear dynamics, with applications to paleoclimatic time series', *Physica D: Nonlinear Phenomena* **35**(3), 395–424.
URL: *https://doi.org/10.1016/0167-2789(89)90077-8*

Veeramony, J. & Svendsen, I. (2000), 'The flow in surf-zone waves', *Coastal Engineering* **39**(2-4), 93–122.
URL: *https://doi.org/10.1016/s0378-3839(99)00058-7*

Vittori, G. & Verzico, R. (1998), 'Direct simulation of transition in an oscillatory boundary layer', *Journal of Fluid Mechanics* **371**, 207–232.
URL: *https://doi.org/10.1017/s002211209800216x*

Vreugdenhil, C. (2006), 'Appropriate models and uncertainties', *Coastal Engineering* **53**(2-3), 303–310.
URL: *https://doi.org/10.1016/j.coastaleng.2005.10.017*

Warner, J. C., Sherwood, C. R., Signell, R. P., Harris, C. K. & Arango, H. G. (2008), 'Development of a three-dimensional, regional, coupled wave, current, and sediment-transport model', *Computers and Geosciences* **34**(10), 1284 – 1306. Predictive Modeling in Sediment Transport and Stratigraphy.
URL: *http://www.sciencedirect.com/science/article/pii/S0098300408000563*

Waterhouse, A. F., Valle-Levinson, A. & Winant, C. D. (2011), 'Tides in a system of connected estuaries', *Journal of Physical Oceanography* **41**(5), 946–959.

WAVEWATCH III Development Group (2016), User manual and system documentation of WAVEWATCH III version 5.16, Technical Report Tech. Note 329, NOAA/NWS/NCEP/MMAB, College Park, MD, USA.

Weather2 (2019), 'Wind, wave and weather reports, forecasts and statistics worldwide'. [last accessed: 10/03/2019].
URL: *http://www.myweather2.com/City-Town/United-States-Of-America/California/San-Pablo-Bay/climate-profile.aspx?month=12*

Web of Science (2019), 'Offshore wind publication topic, between 1980 and 2019'.
URL: *www.webofknowledge.com*

Wegen, M., Dastgheib, A., Jaffe, B. E. & Roelvink, D. (2010), 'Bed composition generation for morphodynamic modeling: case study of san pablo bay in california, USA', *Ocean Dynamics* **61**(2-3), 173–186.
URL: *https://doi.org/10.1007/s10236-010-0314-2*

Wei, G., Kirby, J. T., Grilli, S. T. & Subramanya, R. (1995), 'A fully nonlinear boussinesq model for surface waves. Part 1. Highly nonlinear unsteady waves', *Journal of Fluid Mechanics* **294**, 71–92.
URL: *https://doi.org/10.1017/s0022112095002813*

Westerink, J. J. (2003), 'Development of the governing equations at a point for a turbulent time-averaged continuum'.
URL: *https://coast.nd.edu/jjwteach/www/www/344/PsNotes/topic1_4.pdf*

Whitehouse, R., Bassoullet, P., Dyer, K., Mitchener, H. & Roberts, W. (2000), 'The influence of bedforms on flow and sediment transport over intertidal mudflats', *Continental Shelf Research* **20**(10-11), 1099–1124.
URL: *https://doi.org/10.1016/s0278-4343(00)00014-5*

Wijnberg, K. & Holman, R. (2007), Video-observations of shoreward propagating accretionary waves, *in* C. Dohmen - Janssen & S. Hulscher, eds, 'River, Coastal and Estuarine Morphodynamics, RCEM 2007, 17-21 September 2007, Enschede, The Netherlands, Vol II', Taylor and Francis, United Kingdom, pp. 737–743.

Wijnberg, K. M. & Terwindt, J. H. (1995), 'Extracting decadal morphological behaviour from high-resolution, long-term bathymetric surveys along the holland coast using eigenfunction analysis', *Marine Geology* **126**(1-4), 301–330.
URL: *https://doi.org/10.1016/0025-3227(95)00084-c*

Wilcox, D. C. (1993), *Turbulence modelling for CFD*, DCW Industries, La Cañada.

Williams, J. J., Carling, P. A., Amos, C. L. & Thompson, C. (2008), 'Field investigation of ridge–runnel dynamics on an intertidal mudflat', *Estuarine, Coastal and Shelf Science* **79**(2), 213–229.
URL: *https://doi.org/10.1016/j.ecss.2008.04.001*

Willmott, C. J. (1981), 'ON THE VALIDATION OF MODELS', *Physical Geography* **2**(2), 184–194.
URL: *https://doi.org/10.1080/02723646.1981.10642213*

Winant, C. D., Inman, D. L. & Nordstrom, C. E. (1975), 'Description of seasonal beach changes using empirical eigenfunctions', *Journal of Geophysical Research* **80**(15), 1979–1986.
URL: *https://doi.org/10.1029/jc080i015p01979*

Windfinder (2019), 'Coastal storms'. [last accessed: 10/03/2019].
URL: *https://www.windfinder.com/windstatistics/davis_point_san_pablo_bay*

Winter, C. (2006), 'Meso-scale morphodynamics of teh Eider estuary: analysis and numerical modelling', *Journal of Coastal Research, SI 39 (Proceedings of the 8th International Coastal Symposium)* pp. 498–503.

Winter, C. (2011), Observations and Modelling of Morphodynamics in Sandy Coastal Environments, PhD thesis, University of Bremen.

Wright, L. & Short, A. (1984), 'Morphodynamic variability of surf zones and beaches: A synthesis', *Marine Geology* **56**(1-4), 93–118.
URL: *https://doi.org/10.1016/0025-3227(84)90008-2*

Xian, G. & Weng, Q., eds (2015), *Remote Sensing Applications for the Urban Environment*, Remote Sensing Applications Series, 1st edn, CRC Press, Inc., Boca Raton, FL, USA.

Yacobi, Y. Z., Gitelson, A. & Mayo, M. (1995), 'Remote sensing of chlorophyll in Lake Kinneret using high spectral-resolution radiometer and Landsat TM: Spectral features of reflectance and algorithm development', *Journal of Plankton Research* **17**, 2155–2217.

Zhu, S.-P. & Mitchell, L. (2009), 'Diffraction of ocean waves around a hollow cylindrical shell structure', *Wave Motion* **46**(1), 78–88.
URL: *https://doi.org/10.1016/j.wavemoti.2008.09.001*

Zijlema, M., Stelling, G. & Smit, P. (2011), 'Swash: An operational public domain code for simulating wave fields and rapidly varied flows in coastal waters', *Coastal Engineering* **58**(10), 992 – 1012.
URL: *http://www.sciencedirect.com/science/article/pii/S0378383911000974*

Zoppou, C. & Roberts, S. (1999), 'Catastrophic collapse of water supply reservoirs in urban areas', *Journal of Hydraulic Engineering* **125**(7), 686–695.